Open access • Journal Article • DOI:10.1086/382122

Magnetic reconnection and mass acceleration in flare-coronal mass ejection events

Jiong Qiu, Haimin Wang, Chio-Zong Cheng, Dale E. Gary

Institutions: New Jersey Institute of Technology, Princeton Plasma Physics Laboratory

Published on: 01 Apr 2004 - The Astrophysical Journal (IOP Publishing Ltd.)

Topics: Nanoflares, Solar flare, Magnetic reconnection, Flare and Corona

The Astrophysical Journal, 604:900–905, 2004 April 1

MAGNETIC RECONNECTION AND MASS ACCELERATION IN FLARE–CORONAL MASS EJECTION EVENTS

Jiong Qiu,[1] Haimin Wang,[1] C. Z. Cheng,[2] and Dale E. Gary[1]
Received 2003 November 3; accepted 2003 December 17

ABSTRACT

An observational relationship has been well established among magnetic reconnection, high-energy flare emissions and the rising motion of erupting flux ropes. In this paper, we verify that the rate of magnetic reconnection in the low corona is temporally correlated with the evolution of flare nonthermal emissions in hard X-rays and microwaves, all reaching their peak values during the rising phase of the soft X-ray emission. In addition, however, our new observations reveal a temporal correlation between the magnetic reconnection rate and the directly observed acceleration of the accompanying coronal mass ejection (CME) and filament in the low corona, thus establishing a correlation with the rising flux rope. These results are obtained by examining two well-observed two-ribbon flare events, for which we have good measurements of the rise motion of filament eruption and CMEs associated with the flares. By measuring the magnetic flux swept through by flare ribbons as they separate in the lower atmosphere, we infer the magnetic reconnection rate in terms of the reconnection electric field $E_{\rm rec}$ inside the reconnecting current sheet (RCS) and the rate of magnetic flux convected into the diffusion region. For the X1.6 flare event, the inferred $E_{\rm rec}$ is ~5.8 V cm^{-1} and the peak mass acceleration is ~3 km s^{-2}, while for the M1.0 flare event $E_{\rm rec}$ is ~0.5 V cm^{-1} and the peak mass acceleration is 0.2–0.4 km s^{-2}.

Subject headings: Sun: activity — Sun: coronal mass ejections (CMEs) — Sun: flares — Sun: magnetic fields

1. INTRODUCTION

Coronal mass ejections (CMEs; Hundhausen et al. 1984; Hundhausen 1993) and solar flares are among the most spectacular phenomena of the Sun. Several decades of observations have shown that flares and CMEs are often two aspects of the same eruptive event, although their relationship has been the subject of intense debate (see reviews by Low 1996; Hundhausen 1999). Recent case studies of flares, filament eruptions, and CMEs indicated that fast acceleration of CMEs occurs during the flare impulsive phase (Zhang et al. 2001; Gallagher, Lawrence, & Dennis 2003; Wang et al. 2003; Cheng et al. 2003). These observations suggest that magnetic reconnection plays an important role in the mass acceleration at the early stage of CMEs.

In many theoretical models, the CME is considered as an erupting flux rope (Low 1994; Forbes & Priest 1995; Chen 1989; Amari et al. 2000). The plasma in the closed field lines immediately surrounding the flux rope radiates white light as the CME frontal loop. In some observations, an Hα filament can reside in the lower part of the flux rope. Eruption of the flux rope stretches the surrounding magnetic field lines to a nearly open state, and magnetic reconnection takes place between these field lines to form closed post-flare loops below the erupting flux rope. Mikic & Linker (1994), Magara, Shibata, & Yokoyama (1997), and Choe & Cheng (2000) developed a bipolar sheared-arcade reconnection model to also explain the formation of a flux rope. When the arcade field is sheared above a critical level, a current sheet is formed in a bipolar magnetic arcade, and magnetic reconnection takes place in the current sheet. As a result, a flux rope is formed above the reconnecting current sheet (RCS), and the flare is produced below the current sheet. As the magnetic reconnection progresses, the flux rope rises in height, which further enhances the magnetic reconnection rate. In the breakout model developed by Antiochos, DeVore, & Klimchuk (1999), a sheared arcade rises to reconnect with overlying magnetic fields of opposite polarity, which pushes away the overlying fields and lets the sheared-arcade flux escape. Although a quadrupolar field is required in the breakout model, the inner sheared arcade in this model would evolve very similarly to the bipolar flux ropes. Recently, theoretical calculations by Lin & Forbes (2000) and numerical simulations by Cheng et al. (2003), although based on different models, both show that enhanced mass acceleration is accompanied by an enhanced magnetic reconnection rate in terms of the electric field inside the RCS.

To make further progress in understanding the relationship between flare emission and CME motion, we need to obtain the magnetic reconnection rate based on observations. The magnetic reconnection rate can be determined observationally in well-observed two-ribbon flares, which often exhibit horizontal expansion motion of the ribbons as a result of magnetic reconnection at progressively higher altitudes in the corona (see review by Švestka & Cliver 1992). With a two-dimensional approximation of a bipolar arcade, the electric field inside the RCS can be inferred by measuring the expansion speed of the well-defined ribbon fronts and the magnetic fields that the ribbons sweep through (Forbes & Priest 1984; Forbes & Lin 2000; Poletto & Kopp 1986; Qiu et al. 2002; Wang et al. 2003). More generally, we can measure the magnetic flux swept by the initially appearing ribbon fragments, which is equal to the newly connected magnetic flux at the coronal reconnection site (Fletcher & Hudson 2001; Tarbell, Gaeng, & Saba 2003). Combining these efforts with the study of CMEs is expected to yield interesting insight into the flare-CME relationship.

[1] Center for Solar Research, Physics Department, New Jersey Institute of Technology, 323 Martin Luther King Boulevard, Newark, NJ 07102-1982; qiuj@plage.njit.edu.
[2] Princeton Plasma Physics Laboratory, Princeton University, Princeton, NJ 08543.

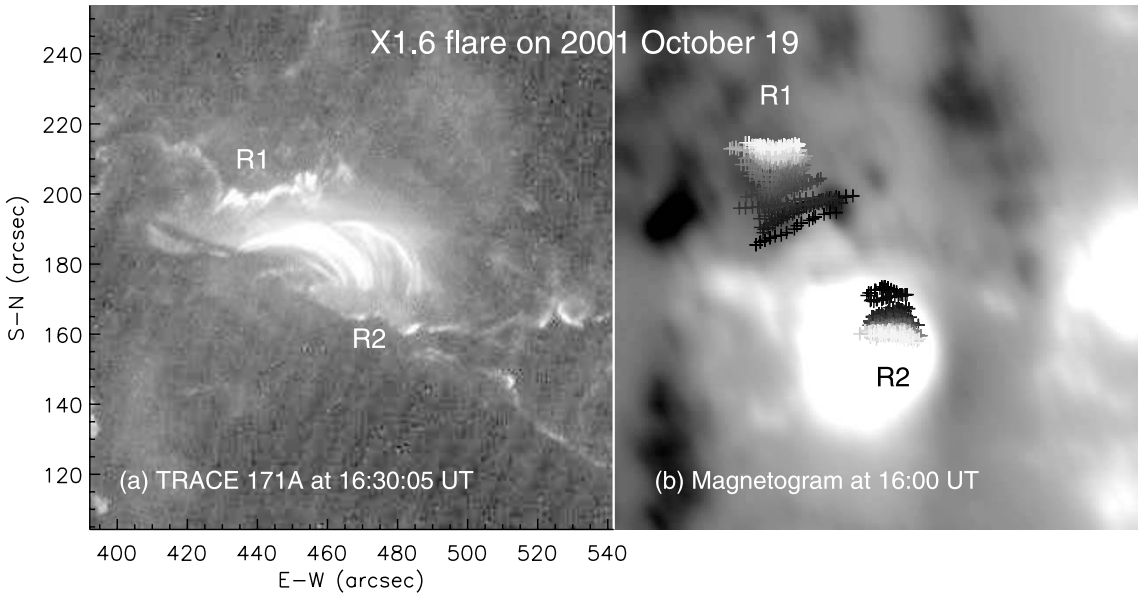

FIG. 1.—(*a*) Snapshot of the X1.6 flare on 2001 October 19 observed by *TRACE* at 171 Å. (*b*) MDI magnetogram of the active region NOAA AR 9661 with the trajectories of the two ribbons superposed. The color of the trajectories from dark to white indicates a 30 minute time lapse from 19:10 to 19:40 UT.

In this paper, we analyze eruptive two-ribbon flares associated with CMEs to study the relationship between magnetic reconnection rate and mass acceleration. The two flares discussed in this paper are also associated with filament eruptions, and we measure the rising motion of the filaments as a signature of flux-rope motion and coronal mass ejections.

2. OBSERVATIONS

We analyze two flare-CME events that were observed by several instruments at different wavelengths. An X1.6 flare occurred in NOAA Active Region 9661 (N15, W29) at 16:25 UT on 2001 October 19. It is accompanied by filament eruption and a fast halo CME. For this flare, *Transition Region and Coronal Explorer* (*TRACE*) observations at 171 Å were acquired with a 30 s cadence, which are used to measure the ribbon expansion and filament rising motion. Figure 1 shows the flare at 171 Å and the magnetogram.

The other event in this study consists of an M1.0 flare, an erupting filament, and a fast halo CME. The flare occurred in a decaying active region (S12, W18) at 11:40 UT on 2000 September 12. It is a long duration event, with the bright ribbons seen in Hα for over 2 hr. For this event, we use observations from the Global Hα Network at Kanzehohe Solar Observatory (KSO) in Austria to measure the ribbon expansion. Figure 2 shows the flare observed in Hα and the magnetogram. EUV images obtained by the *Solar and Heliospheric Observatory* (*SOHO*) EUV Imaging Telescope (EIT) are used to trace the filament rising motion. Wang et al.

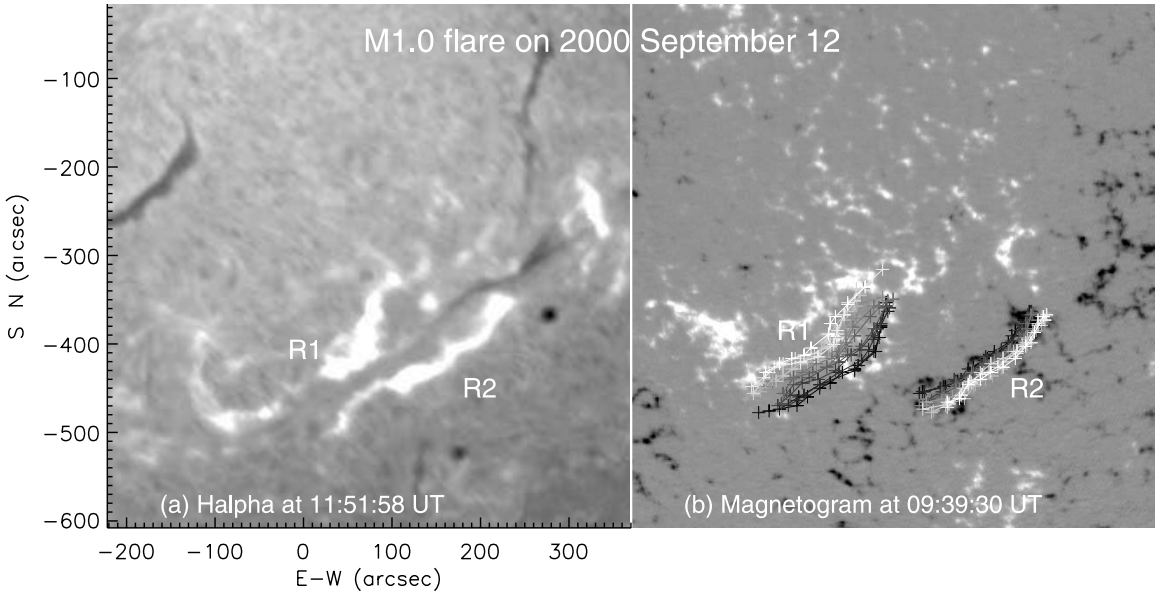

FIG. 2.—(*a*) Snapshot of the M1.0 flare on 2000 September 12 observed by KSO in Hα. (*b*) MDI magnetogram of the active region with the trajectories of the ribbon fronts superposed. The color of the trajectories from dark to white indicates a 2 hr time lapse from 11:00 to 13:00 UT.

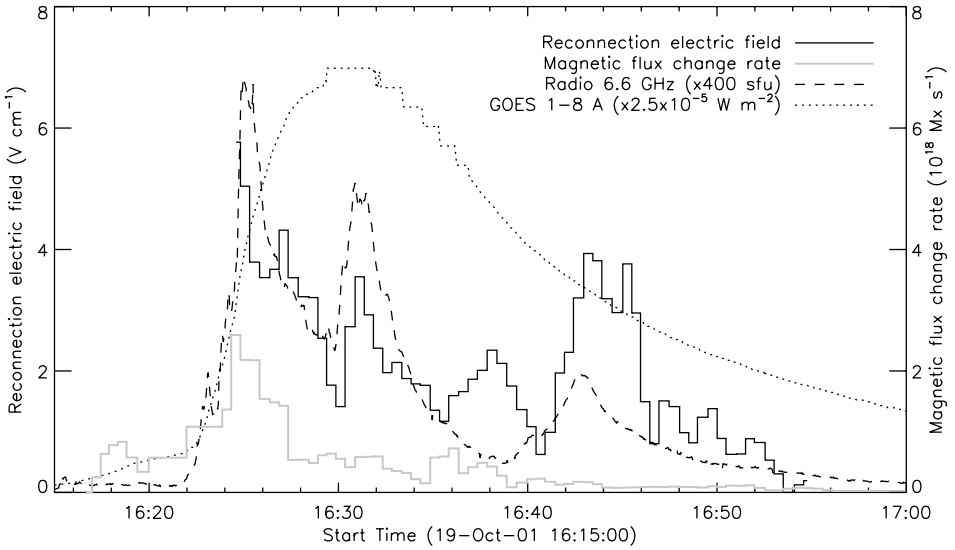

FIG. 3.—Reconnection electric field $E_{\rm rec}$ and magnetic flux change rate $\varphi_{\rm rec}$ derived for the X1.6 flare on 2001 October 19 compared with the soft X-ray and microwave light curves.

(2003) studied the evolution of the filament, CME, and flare ribbon separation of this event. In this paper, we revisit this event with a careful comparison of the magnetic reconnection rate to the evolution of the mass ejection.

Measurements of the CME height are released at the *SOHO* LASCO Web site.[3] We also collect X-ray and microwave observations for these events. Soft X-ray observations by *GOES* were obtained for both events. For the X1.6 event, microwave observations were obtained by the Owens Valley Solar Array (Gary & Hurford 1990), and hard X-ray observations were obtained by *Yohkoh*. No hard X-ray and microwave observations were found for the M1.0 event, and we thus use the time derivative of the *GOES* soft X-ray light curve to indicate the evolution of flare nonthermal emission by assuming that the Neupert effect (Neupert 1968; Dennis & Zarro 1993) holds for this flare.

3. RESULTS

We measure the magnetic reconnection rate in two forms, the reconnection electric field $E_{\rm rec}$ and the rate of magnetic flux change $\varphi_{\rm rec}$. Methods and uncertainties of these measurements are extensively discussed by J. Qiu et al. (2003, in preparation). We measure the expansion velocity V_r of well-defined flare ribbons and the normal component of the magnetic fields B_n they sweep through, and $E_{\rm rec}$ is then given by $E_{\rm rec} = V_r B_n$. For both events, we measure the expansion speed of two evident ribbons that can be traced unambiguously at either side of the magnetic inversion line throughout the flare. Since both flares occur near the disk center, we approximate B_n with the longitudinal component of the magnetic fields that are extrapolated to 2000 m above the photosphere using the Michelson Doppler Imager (MDI) photospheric magnetograms taken before the flares. The electric field is inferred in each of the two ribbons as $E_1 = V_{r1} B_{n1}$ and $E_2 = V_{r2} B_{n2}$, and we average E_1 and E_2 to obtain the mean reconnection electric field $E_{\rm rec}$. The time profile of $E_{\rm rec}$ is plotted in Figures 3 and 4 for the two events, respectively.

[3] For more information, see: http://cdaw.gsfc.nasa.gov/CME_list/.

To derive the rate of magnetic flux change, we apply a numerical method that counts all the newly brightened areas dA at each time with respect to the previous time, and integrate the magnetic flux over dA to obtain $\varphi_{\rm rec} = \partial/\partial t\left(\int B_n dA\right)$. This method avoids the difficulty in determining the velocities of the ribbons, which usually do not have a regular shape. Therefore, it can be applied to images at the early stage of the flare as well, whereas with the first method we can start measurements only after the ribbons are properly formed. The rate of magnetic flux change (in absolute value) is measured for each of the two ribbons as φ_1 and φ_2, respectively: we then take the mean of φ_1 and φ_2 as the flux change rate $\varphi_{\rm rec}$. Figures 3 and 4 show the time profile of $\varphi_{\rm rec}$ for the two events, respectively.

In Figures 3 and 4, we also compare the inferred magnetic reconnection rate with flare emissions at X-ray and microwave wavelengths for the X1.6 and M1.0 events, respectively. It is seen that $E_{\rm rec}$ and $\varphi_{\rm rec}$ have very similar time profiles that are also correlated with the microwave light curve and the time derivative of the soft X-ray light curve. In both events, the magnetic reconnection rate and flare nonthermal emission achieve their maximum values nearly coincidently during the rise of soft X-ray emission. Specifically, for the X1.6 event (Fig. 3) microwave emissions peak at 16:25 UT, when we also find the maximum $E_{\rm rec}$ of ~5.8 V cm^{-1}, and the maximum $\varphi_{\rm rec}$ of order 3×10^{18} Mx s^{-1}. For the M1.0 flare (Fig. 4), the maxima of $E_{\rm rec}$ (~0.5 V cm^{-1}) and $\varphi_{\rm rec}$ (~2×10^{18} Mx s^{-1}) coincide with the maximum of the soft X-ray time derivative, which may resemble time profiles of flare nonthermal emission, at 11:40 UT. The X1.6 event has a larger $E_{\rm rec}$ than the M1.0 event by almost an order of magnitude, which may be a result of the X1.6 flare event occurring in a stronger magnetic field region than the M1.0 event. On the other hand, since the M1.0 event takes place in a much larger region, the integrated magnetic flux change $\varphi_{\rm rec}$ is comparable in the two events.

The good temporal correlation among the time profiles of $E_{\rm rec}$, $\varphi_{\rm rec}$, and flare nonthermal emission suggests that the magnetic reconnection rate governs the energy release in flares, and that the $E_{\rm rec}$ field plays an important role in accelerating nonthermal electrons to emit hard X-rays and microwaves. Such a correlation also justifies using the microwave and hard X-ray light curves and the time derivative of the soft X-ray light

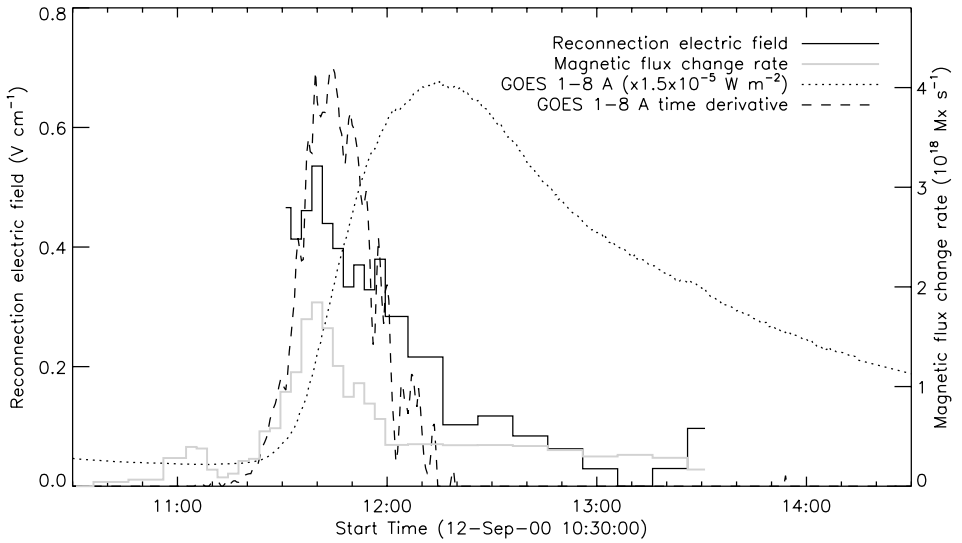

FIG. 4.—Reconnection electric field $E_{\rm rec}$ and magnetic flux change rate $\varphi_{\rm rec}$ derived for the M1.0 flare on 2000 September 12 compared with the soft X-ray light curve and its time derivative.

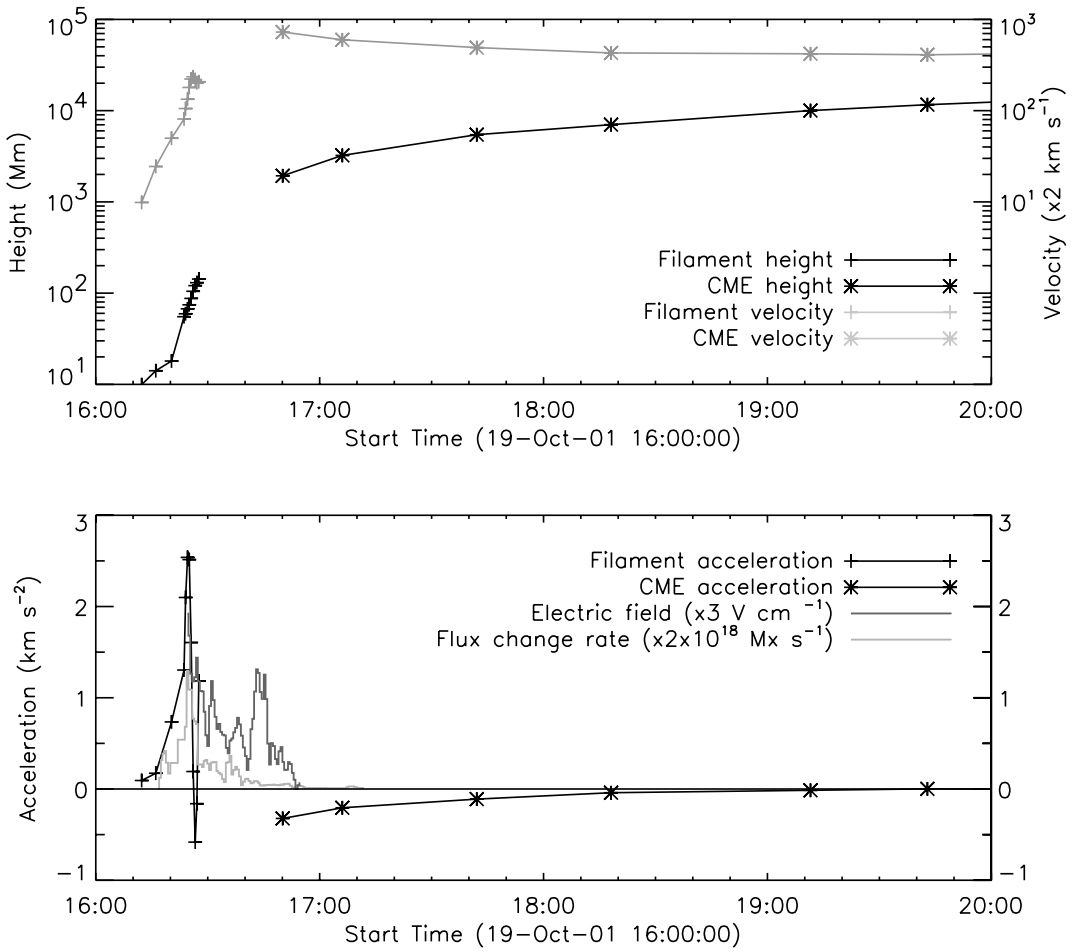

FIG. 5.—Evolution of flare, filament, and CME in the 2001 October 19 event. *Top*: Measured heights and deduced velocities of the filament and CME. *Bottom*: Deduced acceleration of the filament and CME, compared with $E_{\rm rec}$ and $\varphi_{\rm rec}$.

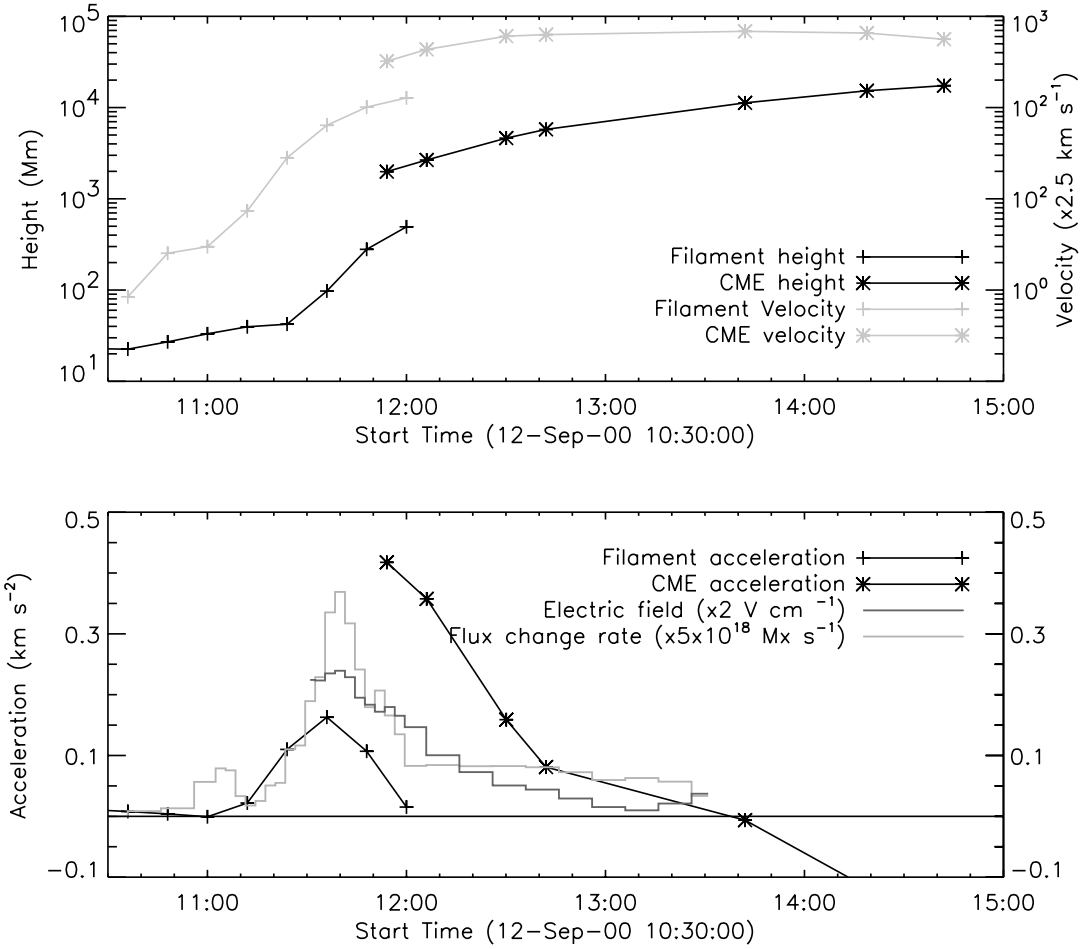

FIG. 6.—Same as Fig. 5, but for the 2000 September 12 event

curve to infer the evolution of the magnetic reconnection rate, as in previous studies (Zhang et al. 2001; Gallagher et al. 2003; Cheng et al. 2003; Wang et al. 2003).

Figures 5 and 6 show the rising motion of the filament and CME in the two events, as compared with $E_{\rm rec}$ and $\varphi_{\rm rec}$. The filament heights are measured from EUV images, and the CME time-height profiles are provided by the LASCO team.[4] The velocity and acceleration of the filament and CME are obtained as the first and second time derivative of the height, respectively, to avoid the dependence on a specific fitting model. We compute the velocity and acceleration for the filament and CME separately because they are different parts of the same entity in the eruption, and might not rise at the same velocity. Note that in the filament and CME measurements we do not correct projection effects, which may give a factor of 2–3 in the number scales in both events, but should not affect the velocity or acceleration time profiles.

Comparing the evolution of the filament and CME with $E_{\rm rec}$ and $\varphi_{\rm rec}$, we find that the mass acceleration and magnetic reconnection have similar evolution profiles. Before the impulsive rise of the flare nonthermal emission, we observe a slow rise of the filament accompanied by small-scale brightenings and a low rate of magnetic flux change from Hα and EUV data. This suggests that magnetic reconnection also plays a role in triggering the eruption. In some CME models, the initial stage reconnection is invoked as a mechanism for the loss of equilibrium (Lin & Forbes 2000; Mikic & Linker 1994) that then leads to the flux-rope eruption. Magnetic reconnection prior to the eruption may also occur with the rise of strongly sheared magnetic core flux in the breakout model (Antiochos et al. 1999), similar to the tether-cutting model (Moore & La Bonte 1980). The fast-rising stage coincides with the flare impulsive phase, and the mass acceleration increases rapidly along with the increase of the magnetic reconnection rate. Within the given temporal resolution, the maximum of the filament/CME acceleration may be regarded as coincident with the peak of $E_{\rm rec}$ and $\varphi_{\rm rec}$. As the magnetic reconnection rate decreases, the mass acceleration also decreases. Around the time when magnetic reconnection ceases, the rising-mass motion slows and the acceleration becomes deceleration. To sum up, in both events there is a close temporal correlation between the mass acceleration and magnetic reconnection within the observing accuracy of about 10 minutes.

The time intervals of magnetic reconnection ($t_{\rm rec}$) and mass acceleration ($t_{\rm acc}$) also reflect a correlation between the two. We estimate the time intervals of the filament and CME acceleration as the time between the rapid takeoff of the filament mass and the deceleration stage, i.e., the duration of positive $a_{\rm fil}$ or $a_{\rm CME}$. For the X1.6 event, the time interval of acceleration is about 30 minutes at the maximum. And for the M1.0 event, the acceleration time interval is over 1 hr for the filament, and at least 2 hr for the CME. These acceleration time intervals in the two events are comparable to the durations of

[4] For more information, see: http://cdaw.gsfc.nasa.gov/CME_list/.

magnetic reconnection, which further suggests that the evolution of the mass ejection and the accompanying flare are closely related.

A comparison of the magnitudes of $E_{\rm rec}$ and $a_{\rm fil}$ or $a_{\rm CME}$ between the two events also hints at a correlation. It is seen that the X1.6 event occurs in a strong magnetic field region and has a large reconnection electric field of order $E_{\rm rec} \approx 6$ V cm^{-1}. The maximum acceleration of the filament mass $a_{\rm fil}$ reaches 2.6 km s^{-2} around the maximum of $E_{\rm rec}$. In contrast, the M1.0 event takes place in a weaker magnetic field region, the maximum reconnection electric field is smaller by an order of magnitude, namely, $E_{\rm rec} \approx 0.5$V cm^{-1} at the peak, and the measured maximum acceleration $a_{\rm fil}$ is less than 0.2 km s^{-2}, and $a_{\rm CME}$ is ~0.4 km s^{-2}, smaller than the X1.6 event by an order of magnitude. Uncertainties in the measurements (Qiu et al. 2003) may affect the values of these quantities, but are unlikely to cause a relative change of an order of magnitude. The measured quantities of mass acceleration and electric field strength are consistent with the calculations by Lin & Forbes (2000), and the values of the X1.6 event are also consistent with the observed mass acceleration and simulated reconnection electric field of an X1.8 flare-CME event on 2000 November 24 reported by Cheng et al. (2003).

Also shown in Figures 5 and 6, the maximum CME velocities in these two events are comparable, being 1450 and 1700 km s^{-1}, respectively. This is because the maximum velocity of the mass ejection is related to both the magnitude and duration of acceleration. Specifically for the two events studied, the filament and CME accompanying the X1.6 event have a larger acceleration than those accompanying the M1.0 event, but for a shorter time.

4. CONCLUSIONS

In this paper, we present the magnetic reconnection rate obtained from the measurement of the rate of change in magnetic flux in two-ribbon flares. The inferred reconnection rate is compared with the rising motion of filaments and CMEs associated with the flares. We obtain the magnetic reconnection rate in terms of the electric field $E_{\rm rec}$ in the RCS by measuring the expansion velocity of the flare ribbons and the magnetic fields the ribbons sweep through at the chromosphere. Taking into account the spatial scale of the system, the magnetic reconnection rate can also be measured in terms of the magnetic flux rate $\varphi_{\rm rec}$ convected into the diffusion region in the RCS.

We find that there is a temporal correlation among $E_{\rm rec}$, $\varphi_{\rm rec}$, and mass (filament and CME) acceleration ($a_{\rm fil}$ and $a_{\rm CME}$) in both events studied in this paper. With the observing time resolution of ~10 minutes, they rise, peak, and decay simultaneously. The time profile of $E_{\rm rec}$ also correlates well with the flare nonthermal emission; both peak during the rise of soft X-ray emission. Our results clearly indicate that the physical link between the evolution of flares and CMEs is magnetic reconnection. Observations of the two events also support the idea that a stronger reconnection electric field, which is equivalent to a greater magnetic reconnection rate per unit length along the arcade, is associated with a greater mass acceleration. In particular, for the X1.6 and M1.0 events presented in this paper the maximum $E_{\rm rec}$ are 5.8 and 0.5 V cm^{-1}, and the corresponding maximum mass accelerations are 2.6 and 0.2–0.4 km s^{-2}, respectively.

Finally, to improve the statistical significance more events should be analyzed to verify the correlation between the mass acceleration and the magnetic reconnection rate studied in this paper. Moreover, it is important to determine whether other kinds of CME configurations will yield similar relationships between the magnetic reconnection rate and the mass acceleration.

We thank Jun Lin and Gwangson Choe for helpful discussions. We are grateful to the referee for constructive comments and suggestions on our work and manuscript. The CME catalog is generated and maintained by NASA and the Catholic University of America in cooperation with the Naval Research Laboratory. *SOHO* is a project of international cooperation between ESA and NASA. This work is supported by the NSF grant AST-0307670 and NASA grant NAG5-10212. C. Z. C. is supported by the DoE Contract DE-AC02-76-CHO3073.

REFERENCES

Amari, T., Luciani, J. F., Mikic, Z., & Linker, J. 2000, ApJ, 529, L49
Antiochos, S. K., DeVore, C. R., & Klimchuk, J. A. 1999, ApJ, 510, 485
Chen, J. 1989, ApJ, 338, 453
Cheng, C. Z., Ren, Y., Choe, G. S., & Moon, Y.-J. 2003, ApJ, 596, 1341
Choe, G. S., & Cheng, C. Z., 2000, ApJ, 541, 449
Dennis, B. R. & Zarro, D. M. 1993, Sol. Phys., 146, 177
Fletcher, L., & Hudson, H. 2001, Sol. Phys., 204, 69
Forbes, T. G., & Lin, J. 2000, J. Atmos. Sol-Terr. Phys., 62, 1499
Forbes, T. G., & Priest, E. R. 1984, in Solar Terrestrial Physics: Present and Future, ed. D. M. Butler and K. Paradupoulous (NASA), 1
———. 1995, ApJ, 446, 377
Gallagher, P. T., Lawrence, G. R., & Dennis, B. R. 2003, ApJ, 588, 53L
Gary, D. E., & Hurford, G. J. 1990, ApJ, 361, 290
Hundhausen, A. J. 1993, J. Geophys. Res., 98, 13177
———. 1999, in The Many Faces of the Sun: a Summary of the Results from NASA's Solar Maximum Mission, ed. K. T. Strong et al. (New York: Springer), 143
Hundhausen, A. J., Sawyer, C. B., House, L., Illing, R. M. E., & Wagner, W. J. 1984, J. Geophys. Res., 89, 2639
Lin, J., & Forbes, T. G. 2000, J. Geophys. Res., 105, 2375
Low, B. C. 1994, Plasma Phys., 1, 1684
———. 1996, Sol. Phys., 167, 217
Magara, T., Shibata, K., & Yokoyama, T. 1997, ApJ, 487, 437
Mikic, Z., & Linker, J. A. 1994, ApJ, 430, 898
Moore, R. L., & LaBonte, B. 1980, in Proc. Symposium on Solar and Interplanetary Dynamics, ed. M. Dryer & E. Tandberg-Hanssen (Dordrecht: Reidel), 207
Neupert, W. M. 1968, ApJ, 153, L59
Poletto, G., & Kopp, R. A. 1986, in The Lower Atmosphere of Solar Flares, ed. D. F. Neidig (Sunspot: NSO), 453
Qiu, J., Lee, J., Gary, D. E., & Wang, H. 2002, ApJ, 565, 1335
Švestka, Z., & Cliver, E. W. 1992, in Eruptive Solar Flares, ed. Z. Svestka et al. (Berlin: Springer), 1
Tarbell, T., Gaeng, T., & Saba, J. 2003, BAAS, 35, 3
Wang, H., Qiu, J., Jing, J., & Zhang, H. 2003, ApJ, 593, 564
Zhang, J., Dere, K. P., Howard, R. A., Kundu, M. R., & White, S. M. 2001, ApJ, 559, 452